The Effect of Low-molecular-weight Species on Space Charge and Conduction in LDPE

Seung Hyung Lee, Jung-Ki Park
Department of Chemical Engineering, Korea Advanced Institute of Science and Technology, Daejon, Korea

Chang Ryong Lee, and Kwang S. Suh
Department of Material Science, Korea University, Seoul, Korea

ABSTRACT

We have investigated the effect of low-molecular mass species on the space charge behavior such as space charge distribution and electrical conduction of LDPE (low density polyethylene). We also attempted to explain the relationship between the space charge distribution and electrical conduction. The heterocharge, conduction current and effective charge mobility decreased when the low-molecular-mass species in LDPE was removed. It was found that the decrease in conduction current was related to the decrease of heterocharge in LDPE.

1. INTRODUCTION

It is known from early work by Fava [1] and Fischer [2] that the dielectric strength of PE (polyethylene) increases with decreasing melt index, *i.e.*, increasing molecular mass, and hence it may be postulated that the low-molecular mass species in PE constitutes the weak structural unit for dielectric strength. In service, power cables such as extruded polyethylene cables are subjected to their normal operating temperature (70 to 90°C). This condition may lead to local melting of the low-molecular mass species and poor thermal stability. This in turn may, with time, affect the long-term reliability of the cable. It is therefore important in designing a power cable to understand the effect of low-molecular-mass species in PE.

Many results have been reported on the space charge distribution in PE using direct measurement techniques [3–8], and also on the electrical conduction of PE [9–15]. However, little has been said about the effect of low-molecular-mass species on the electrical properties of LDPE (low density polyethylene). In this study, we have investigated the effect of low-molecular-mass species on the space charge and electrical conduction of LDPE and have attempted to explain the relationship between the space charge and electrical conduction.

2. EXPERIMENTAL

2.1. SAMPLE PREPARATION

Commercial LDPE without any additives was used in this study. It was produced by the polymerization of ethylene under high pressure using an organic peroxide compound as the initiator. Its density and melt index are 0.920 g/cm^3 and 2.0 g/10 min, respectively. Chemically modified LDPE (g-PE) was prepared by grafting MAH (maleic anhydride) on LDPE using DCP (dicumyl peroxide) as an initiator. The grafting ratio was 0.5% wt. The grafting reaction was carried out in a twin screw extruder at 180 to 200°C. The preparation and characterization of g-PE has been described in detail in our previous work [16].

The low-molecular-mass species in LDPE was extracted by direct extraction using p-xylene (HPLC grade) as a solvent at various temperatures ranging from 53 to 73°C. The fractions were filtered, washed with fresh p-xylene and then dried in a vacuum oven at 60°C for 48 h. The residues from the extraction of LDPE were designated as R53 to R73 and the extracted low-molecular-mass species (extracts) were designated as E53 to E73 where the number indicates the extraction temperature.

For measurements of charge distributions, sheet samples having 1 mm thickness and 9 cm diameter were prepared by compression molding at 120°C for 10 min using a PET (polyethyleneterephthalate) backing film. Film samples for measurements of conduction currents having $\sim$ 50 μm thickness and 5 cm diameter were also prepared by the same process.

Semiconductive electrodes were used for the measurement of space charge distribution. A semiconductive electrode with a thickness of 170 μm was prepared by curing at 180°C using a hot press. The cured semiconductive film was vacuum-degassed at 80°C for 100 h to remove the residual byproducts which may affect the formation of space charge in PE and then attached to the sample using a hot iron. Degassed 50 μm thick semiconductive films were also used as electrodes for the measurement of conduction current.

2.2. ANALYSIS AND MEASUREMENTS

The molecular weight and the molecular weight distribution of the extracts and the residues were determined by GPC (gel permeation chromatography). We used a Waters 150CV instrument, equipped with two Shodex AT-806MS columns mounted in series. 1,2,4-trichlorobenzene,

1070-9878/97/$3.00

containing 0.025% Santonox R antioxidant, was used as the solvent for the GPC system. The characteristics of the column were calibrated using National Bureau of Standards SRM1476 PE and narrow molecular weight PS standards.

Using an infrared spectrometer (Bomem MB-100) at a resolution of 4 cm^{-1}, the fractions were characterized by the amount and types of branches, double bonds and oxygen-containing groups. Films with a thickness of 0.2 to 0.3 mm for IR measurement were prepared by hot pressing at 120°C. The film thickness was measured by a micrometer and the mean value was obtained from four readings. Concentrations of chemical defects N per 1000 main chain carbon atoms were determined from

$$N = f\frac{A}{d\rho} \tag{1}$$

where d is the film thickness cm, ρ the density in g/cm^3, A the absorbance from the base line, and f a coefficient.

The crystallinity and melting temperature were measured by DSC (differential scanning calorimetry) using a DuPont DSC9900 thermal analyzer. An indium standard was used to calibrate the scale of temperature and melting enthalpy. The degree of crystallinity was calculated from the calorimetric data using 69 cal/g for completely crystalline PE [17].

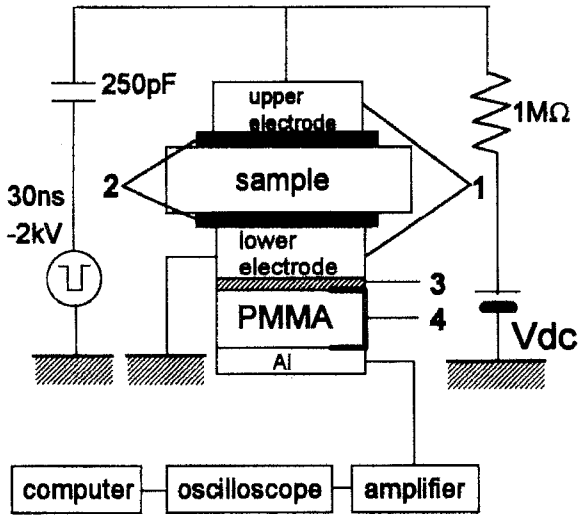

Figure 1. Schematic diagram of PEA instrument for the measurement of space charge distribution. 1: Al electrode, 2: semiconductive electrode, 3: PVDF, 4: Al film.

Charge distributions were measured by a PEA (pulsed electroacoustic) method. The schematic diagram for the experimental apparatus is shown in Figure 1. This experimental apparatus is composed of four parts: pulse generator, power supply, detector including a piezoelectric transducer, and data processing. A electric pulse generator producing a stable source electric pulse with an amplitude of −2 kV and with a duration of 30 ns was used for 1.0 mm thick sample. The piezoelectric detector was made of 28 μm thick PVDF (polyvinylidenefluoride) film. A PMMA (polymethylmethacrylate) block functions as an acoustic absorber which is located below the PVDF film in order to prevent the reflection of the acoustic pressure wave. The upper electrode was designed to allow application of source electric pulse and dc stress at the same time when necessary. The measured signal was calibrated with the area of the calibration peak obtained at 5 kV. When dc voltage is applied to the sample, charge is generated in the sample.

Measurements of charge distributions were carried out as follows. First, the voltage was applied for 30 min across a sample ~ 1 mm thick with semiconductive electrodes. After the voltage application, the sample was short circuited and then immediately the charge distribution was collected. The voltage then was ramped up to the next test voltage. The final voltage was 40 kV, which corresponded to an electric field of ~ 40 kV/mm. In this study, the charge distributions during the voltage application were not measured. Therefore, all the charge distributions described in this paper represent the residual charge remaining in the sample after the discharge.

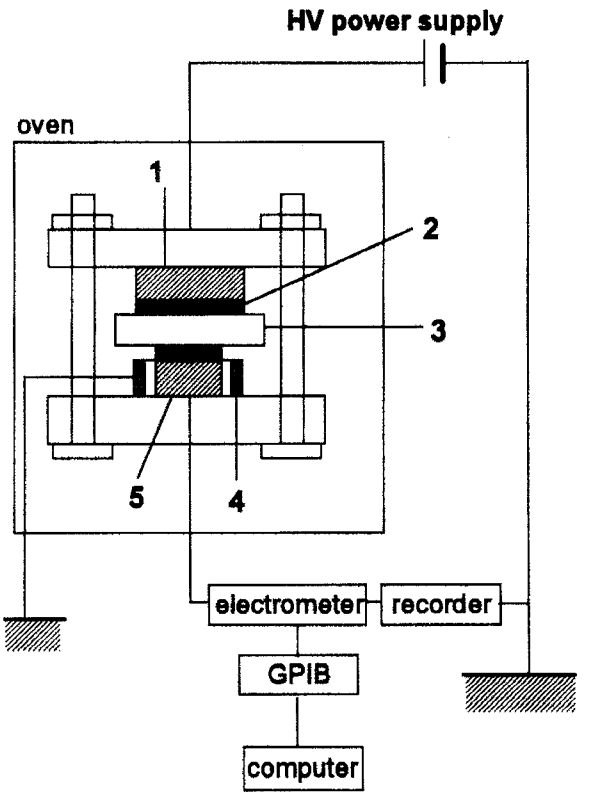

Figure 2. Schematic diagram for measuring the charging current. 1: counter electrode, 2: semiconductive film, 3: sample, 4: guard ring, 5: measuring electrode.

The apparatus used to measure the conduction currents is composed of a power supply (Keithley 247), electrometer (Keithley 617) and test cell (Figure 2). The test cell contains a measuring electrode, the counter electrode, and a guard ring. Tests were carried out at temperatures from 50 to 90°C in an oven and test voltages were adjusted to be in the range to 36 MV/m. Careful attention has been paid in determining the steady state current as a function of charges for a long period of time after the application of dc stress. Only a minor change in its magnitude has been observed after 40 min. The current at 40 min after voltage application was taken as the isochronal current [12].

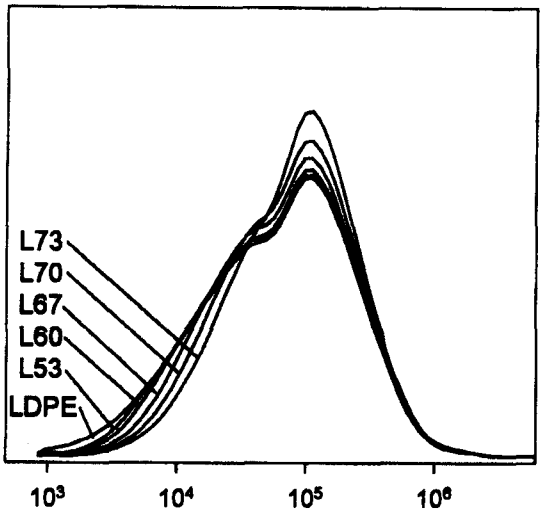

Figure 3. Molecular weight distributions of LDPE and residues.

Table 1. Molecular weights and molecular weight distributions of the various fractions of LDPE.

sample		extract temp. °C	mass fraction %wt	$\overline{M}_n$	$\overline{M}_w$	MWD $\overline{M}_w/\overline{M}_n$
Residue	R53	53	98.5	23790	128400	5.4
	R60	60	96.1	26170	127710	4.9
	R67	67	92.1	31080	131000	4.2
	R70	70	86.3	36000	137300	3.8
	R73	73	72.5	40850	145000	3.5
Extract	R53	53	1.5	2030	6780	3.1
	R60	60	2.4	3750	8600	2.3
	R67	67	4.0	6440	15190	2.4
	R70	70	5.8	9430	20180	2.1
	R73	73	13.8	14800	37640	2.5

3. RESULTS AND DISCUSSION

3.1. FRACTIONATION AND CHARACTERIZATION

Table 1 lists the mass percentage, and the molecular masses $\overline{M}_n$ and $\overline{M}_w$ of the various fractions. Figure 3 shows the MWD (molecular weight distribution) curves of the residues, in which MWD is defined as the ratio of weight average molecular weight to number average molecular weight ($\overline{M}_w/\overline{M}_n$). As shown in Table 1, the average molecular weight of the residue increases and the MWD of the residues decreases with increasing extraction temperature. One can see clearly in Figure 3 that low-molecular-mass species are removed by a xylene extraction of LDPE while the high-molecular-mass species remain almost unchanged. Only the low-molecular-mass species in LDPE are removed as the extraction temperature increases.

The crystallinity and peak melting temperature of the extracts and the residues are summarized in Table 2. The peak melting temperature of the extract increases with increasing molecular mass, and the crystallinity increases to a molecular mass of 15190 (E67), whereas it remains unchanged above 15190.

Table 2. Peak melting temperature and crystallinity of the various fractions of LDPE.

sample		$\overline{M}_w$	Melt temp °C	Cryst %
Residue	R53	128400	110	33
	R60	127710	112	35
	R67	131000	111	34
	R70	137300	111	34
	R73	145000	112	35
Extract	R53	6780	71	19
	R60	8600	88	28
	R67	15190	97	33
	R70	20180	99/103	33
	R73	37640	103/106	33

Table 3 shows the concentrations of structural irregularities such as methyl groups, ketonic carbonyl groups, and three types of carbon-carbon double bonds, terminal vinyl RCH=CH_2, vinylidene RR'C=CH_2, and trans vinylene RCH=CHR', for the residues. It is found that the concentration of chemically irregular parts of the LDPE and the residues decrease as the extraction temperature increases.

3.2. SPACE CHARGE DISTRIBUTIONS

In general, the space charge in LDPE mainly consists of two parts. One is composed of trapped and/or mobile carriers injected from the electrodes [18, 19], dominant under high electric field, and referred to as homocharge [8, 20]. The other comprises the ionization and migration of the organic and inorganic impurities under an electric field [5, 8, 12, 21]. This is the major contributor at low electric fields, and is referred to as heterocharge or bulk space charge.

Figure 4 shows the space charge distribution of the LDPE and the residues after the applied voltage at 40 kV is turned off. Heterocharge was developed in all samples, *i.e.* positive charge near the cathode and negative charge near the anode. The amount of charge near the cathode for the residue decreases as the extraction temperature increases, as shown in Figure 4. These results show that the heterocharge is decreased as more of the low-molecular-mass species are removed from the LDPE. Therefore, we suggest that the heterocharge in the LDPE originates mainly from the low-molecular-mass species.

Most industrial polymers contain various organic and inorganic impurities such as catalysts, antioxidants, residues and byproducts of the crosslinking reaction, *etc.* The dielectric properties of the polymer are probably modified by these impurities. LDPE is not completely nonpolar, because it has impurities originating from the initiators such as air and organic peroxide compounds, and oxygencontaining groups such as ketonic carbonyl groups. These impurities in LDPE come mainly from the low-molecular-mass species in the LDPE and could be polarized under the voltage to form the heterocharge. Therefore, we suggest that the heterocharge in LDPE originates from the migration or polarization of charged low-molecular-mass impurities.

Table 3. Concentrations of structural irregularities (parts/1000 carbon atoms).

sample	Extr. °C	RR'C=O 1720 cm^{-1}	RCH_3 1378 cm^{-1}	RCH=CHR' 964 cm^{-1}	$RCH=CH_2$ 909 cm^{-1}	$RR'C=CH_2$ 888 cm^{-1}
LDPE	-	0.036	30.43	0.071	0.293	0.355
R53	53	0.028	30.62	0.063	0.264	0.331
R60	60	0.019	30.05	0.062	0.231	0.309
R67	67	0.021	28.24	0.058	0.195	0.276
R70	70	0.014	27.01	0.052	0.184	0.263
R73	73	0.011	25.25	0.053	0.176	0.262

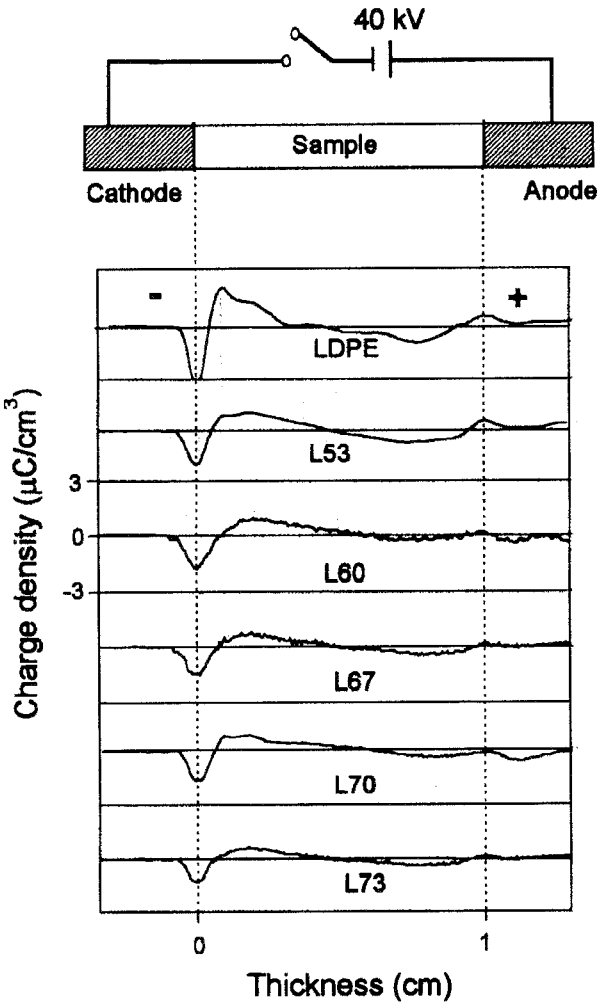

Figure 4. Space charge distribution of LDPE and residues after the applied voltage at 40 kV is turned off.

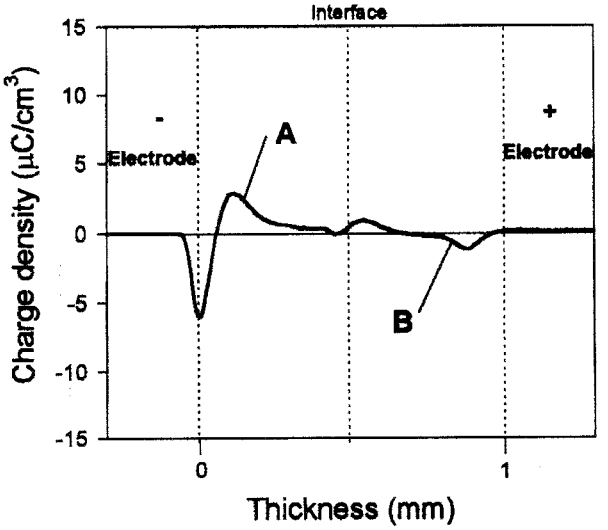

Figure 5. Space charge distribution in double layer laminate of LDPE after the applied voltage at 40 kV is turned off.

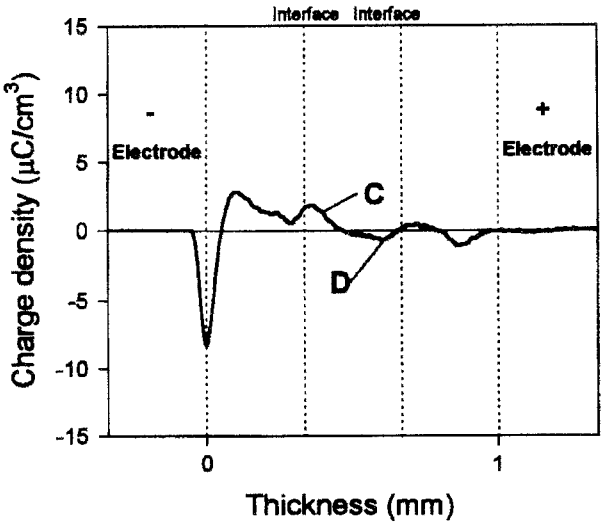

Figure 6. Space charge distribution in triple layer laminate of LDPE after the applied voltage at 40 kV is turned off.

Figures 5 and 6 show the space charge distributions in double and triple layer laminates of LDPE. The polymer/polymer interfaces are located in the laminates. A positive charge peak (A) near the cathode and a negative charge peak (B) near the anode in the double layer laminate of LDPE can be observed in Figure 5. Even though there are interfaces, the charge profiles in the laminates are similar to those in monolayer LDPE shown in Figure 4. In Figure 6, a positive charge peak (C) and a negative charge peak (D) were observed in the central layer of the triple layer laminate of LDPE, which exhibits a heterocharge profile similar to a monolayer LDPE. These figures show that the heterocharges are dominant in each layer of the LDPE laminates and the charge profiles are derived only from LDPE and not from the electrodes, as reported by Li *et al.* [22].

Figures 7 and 8 show the space charge distributions in double and triple layer laminates based on LDPE, the residues and g-PE. Interfacial

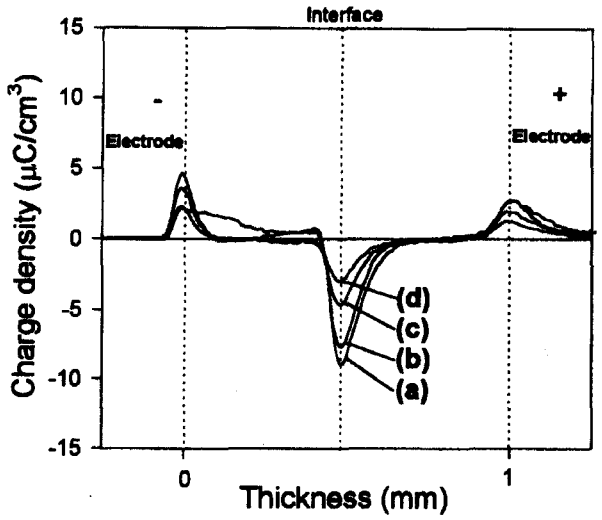

Figure 7. Space charge distributions in double layer laminate based on LDPE, residue and g-PE after the applied voltage at 40 kV is turned off: (a) LDPE (−)/g-PE (+), (b) R53(−)/g-PE(+), (c) R60(−)/g-PE (+), and (d) R70(−)/g-PE (+).

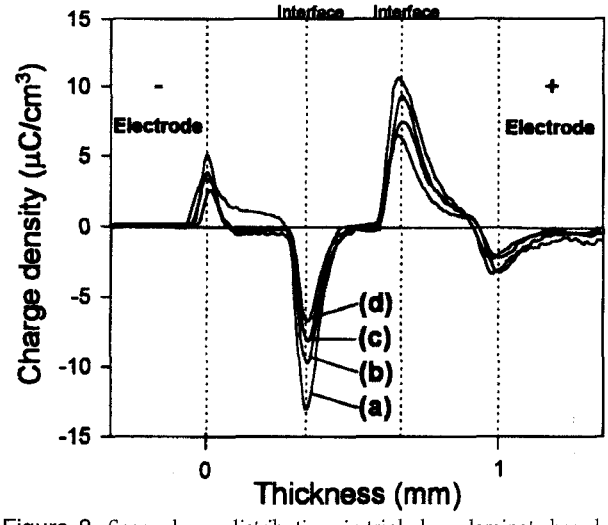

Figure 8. Space charge distributions in triple layer laminate based on LDPE, residue and g-PE after the applied voltage at 40 kV is turned off: (a) LDPE (−)/g-PE /LDPE (+), (b) R60(−)/g-PE /R60(+), (c) R67(−)/g-PE /R67(+), and (d) R70(−)/g-PE /R70(+).

charge peaks are observed at the interfaces in the double and triple layer laminates. It can be seen that the intensities of the interfacial charge peaks decrease with the decrease of low-molecular-mass species in the LDPE. The observation of induced charge peaks at the electrode in Figure 8 indicates that homocharge injects into the LDPE and the residual layer. This suggest that the interfacial charges originate from the heterocharges in the bulk and the injected homocharges from the electrodes. The homocharge injection from the electrodes and the heterocharge transport through the bulk may occur at the same time when a sample is inserted between two electrodes under electric field. The two processes may overlap in space and become inseparable. The type of charge observed may be governed by the process which is dominant at the stage of measurement. Considering the charge trapping effect of g-PE acting as a barrier for charge migration, as presented in our previous work [16, 23], then the injected charges pass through the interface, and some of them may be trapped, giving rise to a charge peak at the interface. We suggest that the decrease of the interfacial charge density in Figures 7 and 8 with removal of the low-molecular mass species results from the decrease of both heterocharge production and homocharge injection. This means that the removal of low-molecular mass species results in the decrease of heterocharges in the bulk and a consequent reduced electric field at the interface between the electrode and the bulk, which in turn decreases the homocharge injection from the electrode.

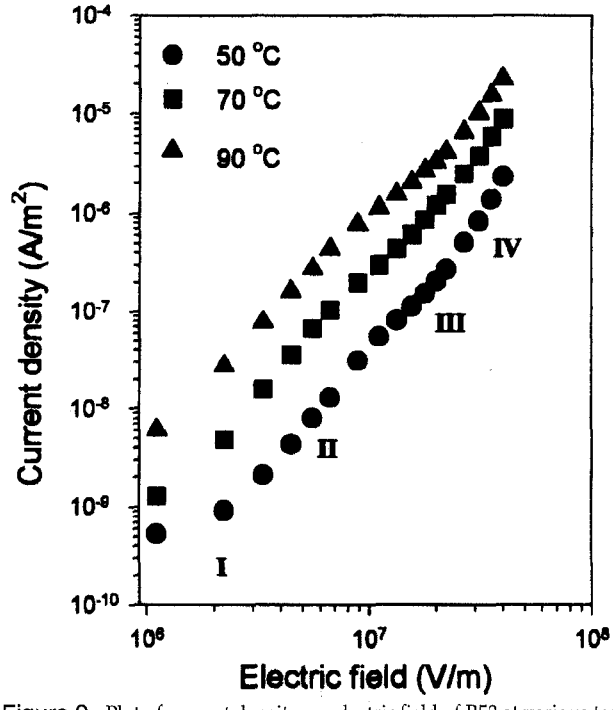

Figure 9. Plot of current density *vs.* electric field of R53 at various temperatures.

3.3. ELECTRICAL CONDUCTION

Equilibrium current density J *vs.* electric field E characteristics for the residues R53 and R67, are shown in Figures 9 and 10. Typically four regions having a different rate of change of current density are observed at 50°C. These are labeled region I, II, III, and IV in the order of increasing electric field. The slopes are $\sim$ 1 for Region I, $\sim$ 2.4 to 2.8 for Region II, $\sim$ 1.8 to 2.2 for Region III, and $\sim$ 2.7 to 3.4 for Region IV.

Figures 11(a) and (b) show the thickness dependence of conduction current of the residues R67 at 50°C and of R70 at 70°C. It is observed that the conduction current is proportional to the -3 power of sample thickness, which is typical for the SCLC (space charge limited conduction) mechanism [24]. In Figures 9 and 10, the slope changes from $\sim$ 1 to $\sim$ 3 at 50°C, which indicates that the conduction mechanism changes from ohmic to SCLC. Above 50°C, however, the SCLC mechanism is shown to be effective over the entire electric field range tested. This kind of observation also was reported in other work [15, 25]. The conduction mechanism for LDPE was also found to be SCLC in our previous work [16]. Therefore, it seems that the conduction mechanism of LDPE remains unchanged after the removal of the low-molecular-mass species.

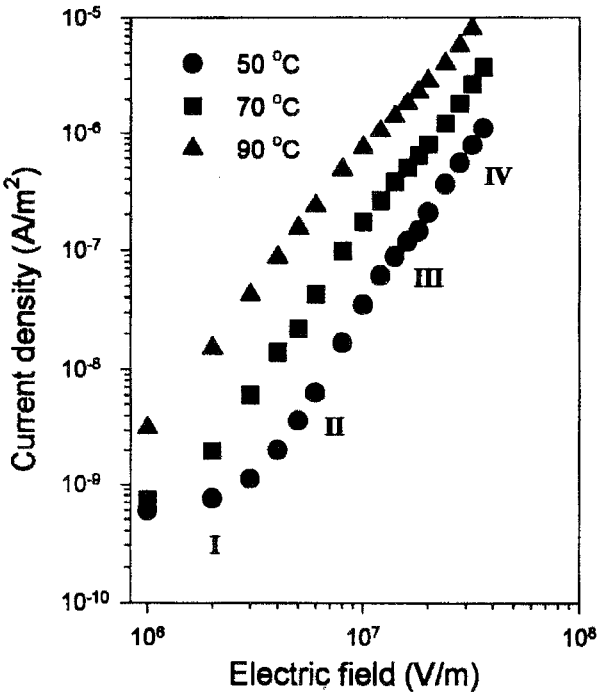

Figure 10. Plot of current density *vs.* electric field of R67 at various temperatures.

Figures 12 and 13 show the equilibrium current density J *vs.* electric field E characteristics for the LDPE and residues at 50°C and 70°C, respectively. The current density of the residue at low electric fields is higher than that of the LDPE, but at high electric fields it becomes lower with increasing extraction temperature. These results are presumably due to the removal of chemically irregular parts as well as other impurities amongst the low-molecular-mass species.

At high electric fields, the current density of the residues decreases as the extraction temperature increases. This may be due to the decrease of chemically irregular parts such as carbonyl groups and carbon-carbon double bonds. The carbonyl groups as oxidation products have a large influence on the electrical conduction of solid polyethylene [13, 14, 26]. For instance, oxidation enhances the conduction current and carrier mobility in LDPE [14]. The carbon- carbon double bonds in PE are also present in low concentration and have little effect on physical properties, but may influence the electrical properties by acting as traps in solid PE [15, 27].

Typical time t dependence of charging currents i is shown in Figures 14(a) and (b), where (a) is for the LDPE and (b) is for the residue (R67). Current maxima in $\log i$ *vs.* $\log t$ curves are observed in LDPE. The current peaks shift to a shorter time when the temperature increases, which is a similar pattern to the transient SCLC peaks proposed by Many and Rakavy [28]. Charge mobilities were calculated from the peak time (arrows in Figure 13(a)) using the equation for the transient SCLC model. They are 4.2×10^{-15} m^2/Vs for 50°C, and 2.3×10^{-14} m^2/Vs for 70°C at 1200 V (24 MV/m) [16].

Figure 14(b) for the residue R67 shows no peaks. No peaks were found for other residues (R53, R70). The reason for this may be that the traps decrease when the chemically irregular parts acting as traps are removed. In the case of SCLC, the effective charge mobility can be calculated from Child's law [26]. Typical values for the residues at 70°C and 1200 V are 8.1×10^{-15} m^2/Vs for R53, 4.1×10^{-15} m^2/Vs for R67, 3.7×10^{-15} m^2/Vs for R70, indicating that the effective charge mobility of the residues decreases when the low-molecular-mass species are removed.

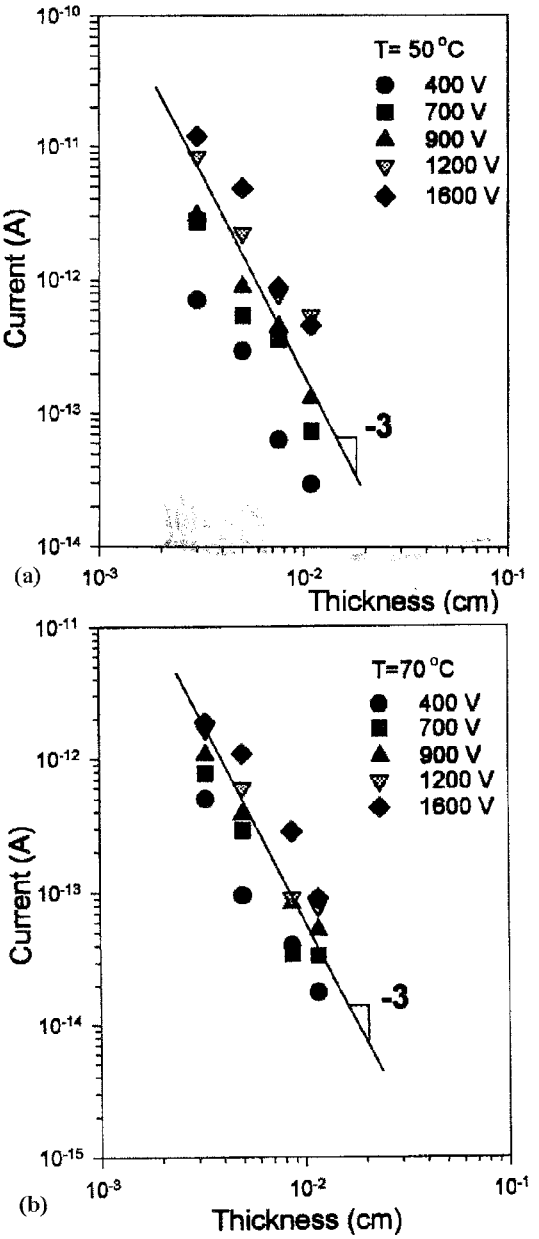

Figure 11. Thickness dependence of conduction currents. (a) R67, (b) R70.

4. CONCLUSIONS

THE heterocharge in LDPE was decreased by removing the low molecular mass species containing chemical impurities The SCLC mechanism which is the main conduction mechanism for LDPE was also effective when low-molecular mass species were removed. The conduction current and effective charge mobility of LDPE at high electric field decreased with removal of the low-molecular-mass species. This might

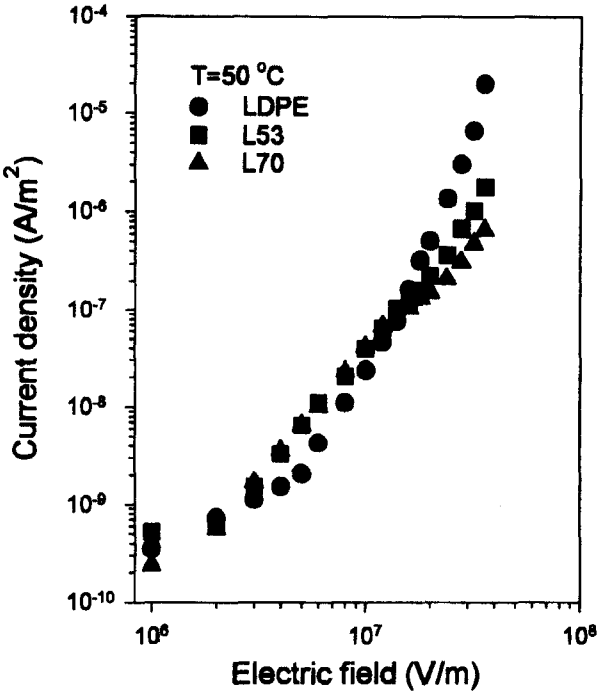

Figure 12. Plot of current density *vs.* electric field of LDPE and residues at 50°C.

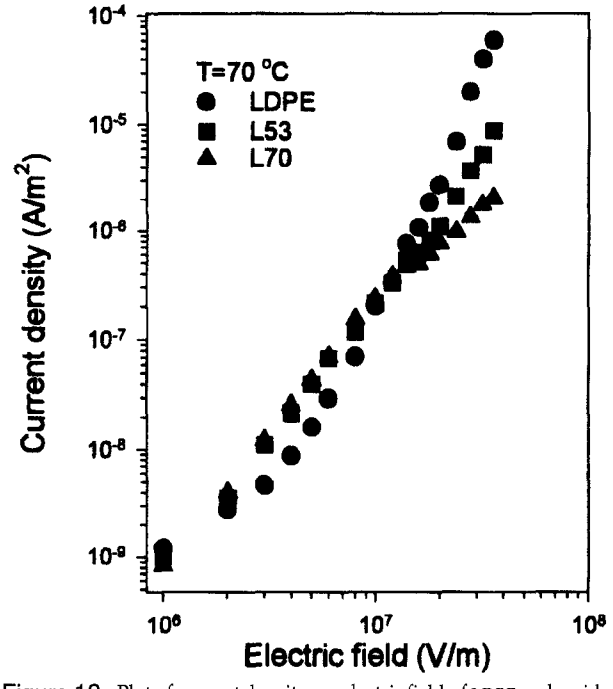

Figure 13. Plot of current density *vs.* electric field of LDPE and residues at 70°C.

be due to the decrease of chemically irregular parts which transport the charges injected from the electrodes into the bulk, and also to the decrease of heterocharge which would result in the reduction of the local electrical field at the interface between electrode and bulk, which in turn would decrease the homocharge injection from the electrodes into the bulk.

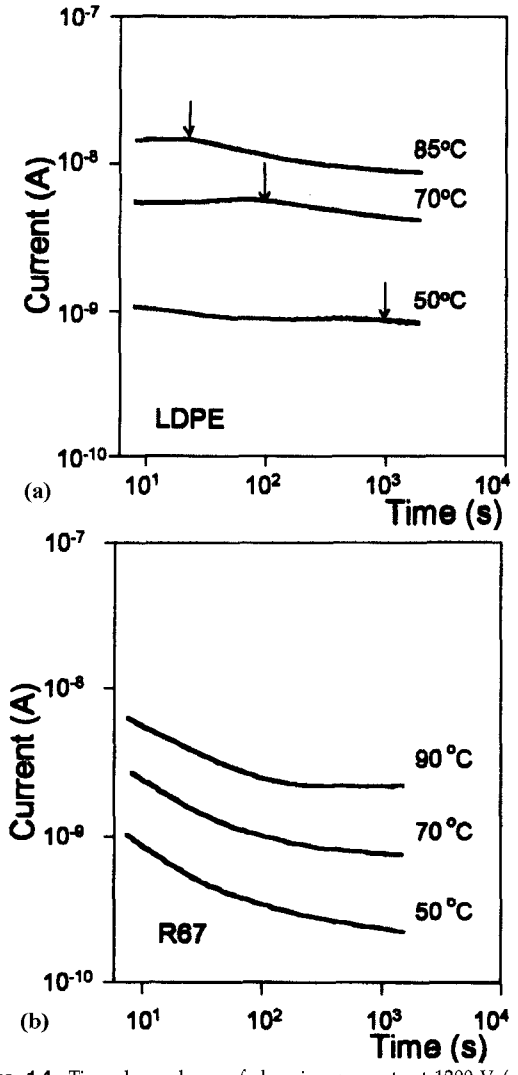

Figure 14. Time dependence of charging currents at 1200 V. (a) LDPE [16], (b) R67.

REFERENCES

[1] R. A. Fava, "Intrinsic Electric Strength and Electromechanical Breakdown in Polyethylene", Proc. IEE 1965, Vol. 112, pp. 819–826, 1965.

[2] P. Fischer, "Electron Transport in Polyethylene", Ann. Rep. CEIDP 1975, National Academy of Sciences, NRC, Washington, DC, pp. 661–664, 1975.

[3] T. Ditchi, C. Alquie, J. Lewiner, E. Favrie and R. Jocteur, "Electrical Properties of Electrode/Polyethylene/Electrode Structure", IEEE Trans. Electr. Insul., Vol. 24, pp. 403–408, 1989.

[4] Y. Suzuoki, T. Furuta, H. Yamada, S. O. Han, T. Mizutani, M. Ieda and N. Yoshifuji, "Study of Space Charge in Polyethylene by Direct Probing: Effect of Oxidation", IEEE Trans. Electr. Insul., Vol. 26, pp. 1073–1079, 1991.

[5] Y. Li, M. Yasuda and T. Takada, "Influence on Spatial Charge Distribution of Crosslinking Agent Residues in XLPE", Proc. 3rd ICPADM, Waseda, Japan, pp. 1210–1215, 1991.

[6] K. Hattori, Y. Suzuoki, T. Mizutani, M. Ieda and T. Suzuki, "Study of Effect of Space Charge on Dielectric Breakdown in Polymers by Laser-Induced-Pressure-Pulse Technique", Proc. 25th Symposium on Electrical Insulating Materials, Nagoya, Japan, pp. 313–316, 1993.

[7] N. Kikuta, H. Hatai, H. Miyata and T. Takahashi, "Effects of Space Charge upon Electrical Conduction", Proc. 25th Symposium on Electrical Insulating Materials, Nagoya, Japan, pp. 297–300, 1993.

[8] Kwang S. Suh, Sun. J. Hwang, Jin. S. Noh and T. Takada, "Effects of Constituents of XLPE on the Formation of Space Charge", IEEE Trans. Dielec. Electr. Insul., Vol. 1, pp. 1077–1083, 1994.

[9] M. Ieda, "Electrical Conduction and Carrier Traps in Polymeric Materials", IEEE Trans. Electr. Insul., Vol. 19, pp. 162–178, 1984.

[10] S. Pelissou, H. St-Onge and M. R. Wertheimer, "Electrical Conduction of Polyethylene below and above Its Melting Point", IEEE Trans. Electr. Insul., Vol. 23, pp. 325–333, 1988.

[11] K. Iida, J. S. Kim, S. Nakamura and G. Sawa, "Effects of Molecular Structure on Electrical Conduction in Low-density Polyethylene above its Melting Point", IEEE Trans. Electr. Insul., Vol. 27, pp. 391–398, 1992.

[12] Kwang S. Suh, Chang. R. Lee, Jin. S. Noh, J. Tanaka and D. H. Damon, "Electrical Conduction in Polyethylene with Semiconductive Electrode", IEEE Trans. Dielec. Electr. Insul., Vol. 1, pp. 224–230, 1994.

[13] T. Mizutani, T. Tsukahara and M. Ieda, "The Effects of Oxidation on the Electrical Conduction of Polyethylene", J. Phys. D: Appl. Phys., Vol. 13, pp. 1673–1679, 1980.

[14] P. Fischer and P. Rohl, "Transient Currents in Oxidized Low-density Polyethylene", Progr. Colloid Polym. Sci., Vol. 62, pp. 149–153, 1977.

[15] P. Fischer, "Electrical Conduction in Polyolefins", J. Electrostat., Vol. 4, pp. 149–173, 1977/1978.

[16] Seung Hyung Lee, Jung-Ki Park, Jae Hong Han and Kwang S. Suh, "Space Charge and Electrical Conduction in Maleic Anhydride Grafted Polyethylene", IEEE Trans. Dielec. Electr. Insul., Vol. 2, pp. 1132–1139, 1995.

[17] P. J. Flory and A. Vrij, "Melting Points of Linear-Chain Homologs. The Normal Paraffin Hydrocarbons", J. Am. Chem. Soc., Vol. 85, pp. 3548–3553, 1963.

[18] W. Xinsheng, H. Yongging and T. Demin, "Trap Density as an Indication of Electrical Aging Degree in Polymer", Proc. 4th ICPADM, Brisbane, Australia, pp. 740–743, 1984.

[19] K. C. Kao, "New Theory of Electrical Discharge and Breakdown in Low-mobility Condensed Insulation", J. Appl. Phys., Vol. 55, pp. 752–755, 1984.

[20] T. Mizutani, "Space Charge Measurement Techniques and Space Charge in Polyethylene", IEEE Trans. Dielec. Electr. Insul., Vol. 1, pp. 923–932, 1995.

[21] Kwang S. Suh, Jung Hoe Koo, Seung Hyung Lee, Jung-Ki Park and T. Takada, "Effect of Sample Preparation Conditions and Short Chains on Space Charge Formation in LDPE", IEEE Trans. Dielec. Electr. Insul., Vol. 3, pp. 153–160, 1996.

[22] Y. Li, T. Takada, H. Miyata and T. Niwa, "Observation of Charge Behavior in Mutiply Low-Density Polyethylene", J. Appl. Phys., Vol. 74, pp. 2725–2730, 1993.

[23] Seung Hyung Lee, Jung-Ki Park, Jae Hong Han and Kwang S. Suh, "Space Charge Behavior in Maleic Anhydride Grafted Polyethylene/ Ethylene-vinylacetate Copolymer Laminates", submitted to J. Phys. D: Appl. Phys. 1995.

[24] M. A. Lampert and P. Mark, *Current Injection in Solids*, Academic Press, New York, 1970.

[25] H. St-Onge, "Electrical Conduction in 3 Percent Carbon-Filled Polyethylene-Part II: High-Field Results", IEEE Trans. Electr. Insul., Vol. 15, pp. 350–358, 1980.

[26] T. Mizutani and M. Ieda, "Carrier Transport in High-Density Polyethylene", J. Phys. D: Appl. Phys., Vol. 12, pp. 291–296, 1979.

[27] T. Tanaka, "Optical Absorption and Electrical Conduction in Polyethylene", J. Appl. Phys., Vol. 44, pp. 2430–2432, 1973.

[28] A. Many and G. Rakavy, "Theory of Transient Space-ChargeLimited Currents in Solids in the Presence of Trapping", Phys. Rev., Vol. 126, pp. 1980–1988, 1962.

Manuscript was received on 24 February 1996, in final form 23 June 1997.